

# Optimization of spin-triplet supercurrent in ferromagnetic Josephson junctions

Carolyn Klose, Trupti S. Khaire, Yixing Wang, W. P. Pratt, Jr., Norman O. Birge\*  
*Department of Physics and Astronomy, Michigan State University, East Lansing, Michigan 48824-2320, USA*

B.J. McMorran, T.P. Ginley,<sup>†</sup> and J.A. Borchers, B.J. Kirby, B.B. Maranville, J. Unguris  
*National Institute of Standards and Technology, Gaithersburg, Maryland 20899, USA*  
 (Dated: August 16, 2021)

In the past year, several groups have observed evidence for long-range spin-triplet supercurrent in Josephson junctions containing ferromagnetic (F) materials. In our work, the spin-triplet pair correlations are created by non-collinear magnetizations between a central Co/Ru/Co “synthetic antiferromagnet” (SAF) and two outer thin F layers. Here we present data showing that the spin-triplet supercurrent is enhanced up to 20 times after our samples are subject to a large in-plane magnetizing field. This surprising result can be explained if the Co/Ru/Co SAF undergoes a “spin-flop” transition, whereby the two Co layer magnetizations end up perpendicular to the magnetizations of the two thin F layers. Direct experimental evidence for the spin-flop transition comes from scanning electron microscopy with polarization analysis and from spin-polarized neutron reflectometry.

PACS numbers: 74.50.+r, 74.45.+c, 75.70.Cn, 74.20.Rp

Experimental and theoretical progress in superconducting/ferromagnetic (S/F) hybrid systems has been impressive over the past decade [1]. When a conventional spin-singlet Cooper pair crosses the S/F interface, the two electrons enter into different spin bands in F with different Fermi wavevectors [2]. The resulting oscillations in the pair correlation function lead to oscillations in several observable quantities [1], but unfortunately the oscillations decay exponentially as soon as the F-layer thickness exceeds the electron mean free path [3].

In contrast to spin-singlet electron pairs, spin-triplet pairs can survive in F as long as they would in a normal metal. While spin-triplet superconductivity arises only rarely in bulk materials [4, 5], it was predicted a decade ago that such pairs can be induced in S/F hybrid systems in the presence of certain kinds of magnetic inhomogeneity involving non-collinear magnetizations [6–8]. Experimental evidence for such spin-triplet pairs was elusive for many years [9, 10]; then, last year, several groups published convincing evidence for spin-triplet supercurrent in S/F/S Josephson junctions containing only conventional spin-singlet S materials [11–14]. The conversion from spin-singlet to spin-triplet pairs was accomplished either by introducing magnetic inhomogeneity artificially, or by relying on a source of inhomogeneity intrinsic to the materials in the samples. In our Josephson junctions, the central F layer is in fact a Co/Ru/Co “synthetic antiferromagnet” (SAF) with the magnetizations of the two Co layers locked anti-parallel to each other by a strong exchange field mediated by the Ru layer (see Fig. 1). We insert additional thin F’ layers on either side of the SAF; these extra layers are crucial to the creation of spin-triplet pairs inside the junctions [15].

What happens when one tries to magnetize the junctions by applying a large in-plane magnetic field? One might expect the critical supercurrent in the junctions to

drop, since the generation of spin-triplet pairs requires the presence of non-collinear magnetization. The main result of this paper is the observation that just the opposite happens. After magnetization, the critical current,  $I_c$ , increases up to a factor 20 relative to its value in the as-grown state. This seemingly counter-intuitive result can be understood by considering a unique property of the SAF: when the large magnetizing field  $H_{app}$  is applied, the Co magnetizations “scissor” towards  $H_{app}$ . When the field is removed, the Co magnetizations relax back to directions perpendicular to  $H_{app}$ . This SAF “spin-flop” transition was predicted and first demonstrated over a decade ago.[16, 17]

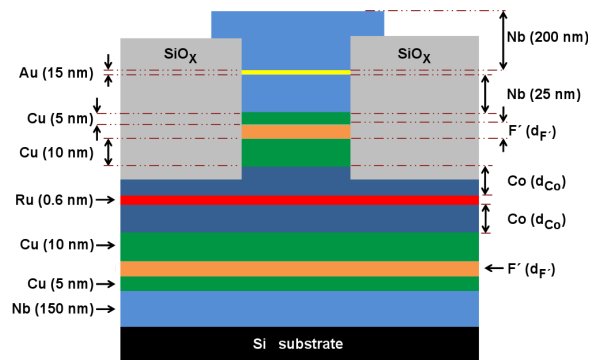


FIG. 1: (color online). Schematic diagram of the Josephson junctions used in the this work, shown in cross-section.

Our sample geometry is illustrated in Fig. 1. The two layers labelled F’ are either pure Ni or Pd<sub>0.88</sub>Ni<sub>0.12</sub> alloy in this work [11, 18]. The inner Cu layers magnetically isolate the F’ layers from the Co layers. The outer Cu layers are present for historical reasons and because

Co grows better on a Nb/Cu buffer layer [19]. The entire multilayer except for the top Nb is sputtered in one run without breaking vacuum. Circular junctions with diameters of 10, 20, and 40  $\mu\text{m}$  are patterned by photolithography and ion milling, followed by deposition of insulating  $\text{SiO}_x$  to isolate the top and bottom Nb leads. Finally the top Nb electrode is sputtered through a mechanical mask. The purpose of the Au layer is to suppress oxidation of the structure during processing; at low temperature the Au becomes superconducting due to the proximity effect with the surrounding Nb layers. The Nb layers start to superconduct just above 9 K; all of the data presented here were obtained at 4.2 K.

The original purpose of the Co/Ru/Co SAF was to provide a strong exchange field for the electrons while simultaneously producing little to no magnetic flux in the junctions. Large-area Josephson junctions containing a strong ferromagnetic material such as Co exhibit complicated and irregular “Fraunhofer patterns” when subject to an applied transverse magnetic field [19, 20]. The irregularities are due to a random pattern of constructive and destructive interference in the gauge-invariant phase difference across the junction caused by the complicated spatial variation of the magnetic vector potential [21]. The presence of the Ru restores textbook-like Fraunhofer patterns centered very close to zero applied field [19], an indication that there is very little intrinsic magnetic flux in the junctions. In this work, the Ru will serve a second, unexpected role, namely to provide a simple way to force the magnetizations of the Co layers to be perpendicular to the magnetizations of the F’ layers.

As background to the new data presented here, we briefly review our previous results [11, 18]. Josephson junctions of the type illustrated in Fig. 1, but without the F’ layers, exhibit a critical supercurrent ( $I_c$ ) that decays rapidly with increasing Co thickness [19]. Defining  $D_{Co}$  as the sum of the thicknesses of the two Co layers, we find that  $I_c \propto \exp(-D_{Co}/l_e)$  with mean free path  $l_e = 2.3\text{nm}$ , for  $D_{Co}$  ranging from 3 to 23 nm. Insertion of the F’ layers with appropriate thicknesses ( $d_{F'}$  between 3 and 6 nm for F’=PdNi, or  $d_{F'}$  between 1 and 2 nm for F’=Ni) enhances  $I_c$  by over two orders of magnitude when  $D_{Co} = 20\text{nm}$ . The dependence of  $I_c$  on  $D_{Co}$  is nearly flat when  $D_{Co}$  varies over the range 12 - 28 nm, with F’=PdNi and  $d_{PdNi} = 4\text{nm}$ . This long-range behavior of the critical supercurrent is the signature of its spin-triplet nature. For the rest of this paper we will focus on samples containing F’ layers of either PdNi or Ni, with  $D_{Co}$  fixed at 20 nm.

Fig. 2 illustrates what happens when samples with F’=Ni and four values of  $d_{Ni}$  are subjected to an applied in-plane magnetic field,  $H_{app}$ . After each value of field is applied, the full Fraunhofer pattern is re-measured in the vicinity of zero field, and we plot the maximum value of  $I_c$  at the central peak of the Fraunhofer pattern. Fig. 2 shows that, at first, very little happens. Then when

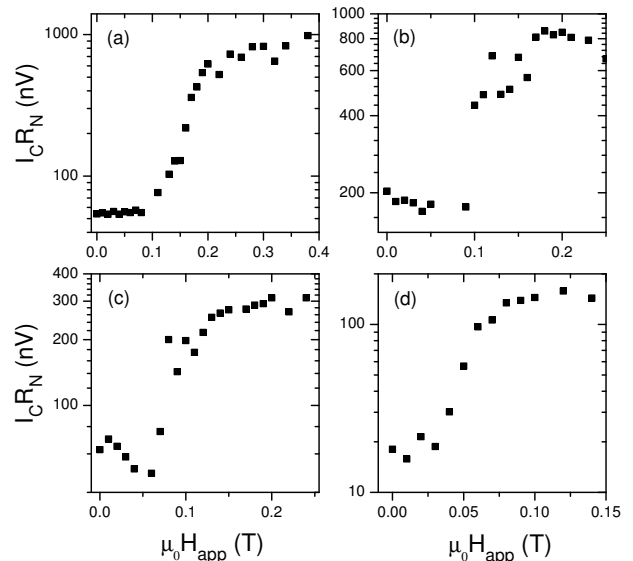


FIG. 2: Critical current times normal-state resistance ( $I_c R_N$ ) as a function of magnetizing field  $H_{app}$  for Josephson junctions containing F’=Ni, for Ni thicknesses  $d_{Ni} = 1.0, 1.5, 2.0,$  and  $2.5$  nm for panels (a)-(d), respectively. Magnetizing the samples enhances  $I_c$  by a large factor that depends on  $d_{Ni}$ . (Uncertainties are dominated by changes in magnetic configuration, and can be estimated from the scatter in the data.)

$H_{app}$  exceeds the coercive field of the Ni layers (in the range of  $\mu_0 H \approx 0.05 - 0.15$  T depending on  $d_{Ni}$ ),  $I_c$  starts to increase dramatically. At large  $H_{app}$ ,  $I_c$  flattens out after having increased by a large factor – up to 20 for  $d_{Ni} = 1.0\text{nm}$ . At the same time, the central peak in the Fraunhofer patterns (not shown) shifts to a small negative field value that is proportional to the Ni thickness, and consistent with the remnant magnetization of our Ni films [22]. The Fraunhofer shifts indicate that the Ni layers are fully magnetized when  $I_c$  saturates in Fig. 2. Similar behavior to that shown in Fig. 2 was found in samples with F’=PdNi with  $d_{PdNi} = 4\text{nm}$ , but in that case the coercive field is larger –  $I_c$  starts to increase only when  $\mu_0 H_{app}$  exceeds 0.15 T, and doesn’t saturate until  $\mu_0 H_{app} = 0.3\text{T}$ . This behavior is consistent with the very large coercive field of PdNi thin films [21]. The Fraunhofer pattern also shifts in the samples with F’=PdNi, but this time by a smaller amount consistent with the remnant magnetization of our PdNi films.

Theory predicts that the spin-triplet supercurrent in our samples is optimized when the magnetizations of the two F’ layers are perpendicular to those of the central Co layers [15, 23, 24]. In fact, no spin-triplet pairs should be generated when all the magnetizations in the sample are collinear. The large enhancement of the critical current shown in Fig. 2 strongly suggests that magnetizing the samples optimizes the orthogonality of the Co magnetizations with respect to the F’ magnetizations. The

small shift of the Fraunhofer pattern, on the other hand, indicates that only the F' layers are magnetized in the direction of  $\mathbf{H}_{app}$ . This scenario is perfectly plausible in the light of the “spin-flop” transition of the SAF [16, 17].

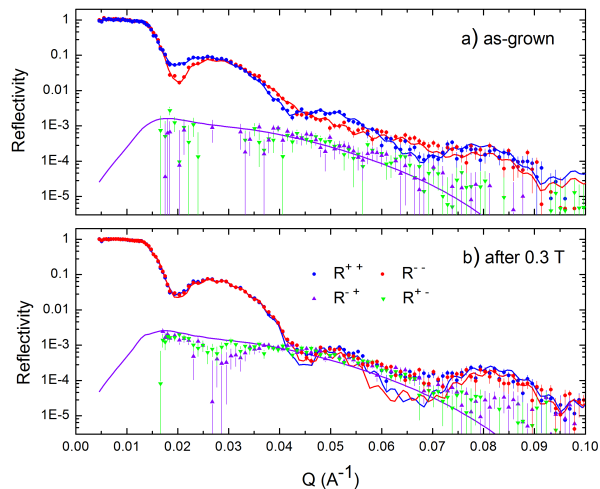


FIG. 3: (color online) Polarized neutron reflectivity data and fits (solid lines) as a function of wavevector  $Q$  from a partial Josephson junction in a small guide field of  $< 0.001$  T a) as-grown and b) after application of a 0.3 T field. The nonspin-flip cross sections,  $R^{++}$  and  $R^{--}$ , correspond to the blue and red circles respectively. The spin-flip cross sections,  $R^{+-}$  and  $R^{-+}$ , correspond to the purple and green triangles.

To identify the magnetic structure responsible for the enhancement of the spin-triplet supercurrent, we made a large-area sample of the form Si/Nb(150 nm)/Cu(10 nm)/Co(6 nm)/Ru(0.6nm)/Co(6nm)/Cu(10 nm), which has the Josephson junction layer structure shown in Fig. 1 through the Cu layer on top of the upper Co layer. The Co magnetizations were characterized with the complementary techniques [25] of specular polarized neutron reflectivity (PNR) and scanning electron microscopy with polarization analysis (SEMPA) at room temperature. (PNR measurements were also performed at low temperature on a different sample, with results similar to those shown here.) PNR nondestructively measures the net in-plane magnetization for each ferromagnetic layer, even in the presence of a field. SEMPA combined with ion milling images the remanent magnetic structure in each layer.

The magnetization of the ferromagnetic layers was first analyzed in the as-grown state. For the PNR measurements, performed on the NG-1 Reflectometer at the NIST Center for Neutron Research, the spin states of the incident and scattered neutrons were selected to produce the nonspin-flip (NSF) cross sections ( $R^{++}$  and  $R^{--}$ ) and the spin-flip (SF) cross sections ( $R^{+-}$  and  $R^{-+}$ ) shown in Figure 3. The NSF scattering is sensitive to the nuclear structure of the sample, and the splitting between

$R^{++}$  and  $R^{--}$  originates from the projection of the magnetization parallel to the guide field ( $< 0.001$  T). The SF scattering is entirely magnetic and arises from the component of the magnetization that is perpendicular to the field. The data were all fit with a model using the *Reflpak* software package [26] to determine the depth-dependence of both the composition and vector magnetization averaged across the  $1 \text{ cm}^2$  area of the sample.

In Fig. 3a), the NSF cross sections are dominated by structural contributions, but the  $R^{++}$  and  $R^{--}$  exhibit a small splitting indicative of a net moment component parallel to the field. The SF scattering is small, but non-zero, consistent with a slight canting of the Co layer magnetizations away from the field. The red arrows in Fig. 4a) and b) represent the average orientation and magnitude of the net magnetizations of the top and bottom Co layers obtained from the PNR fits. SEMPA was then used to image the magnetization of each layer within a  $\approx 1 \text{ mm}^2$  ion-milled window of the same sample. Ion milling with 800 eV Ar ions first reveals the top Co layer magnetization (Fig. 4a), and then the bottom Co layer (Fig. 4b). The distribution of magnetization directions in these images are shown in the corresponding polar plots. Both the PNR and SEMPA measurements indicate a preferred direction for the magnetization in the as-grown state, with most of the magnetization aligned along an angle approximately  $20^\circ$  relative to a sample edge. Both measurements also show antiferromagnetic coupling between the top and bottom Co layers.

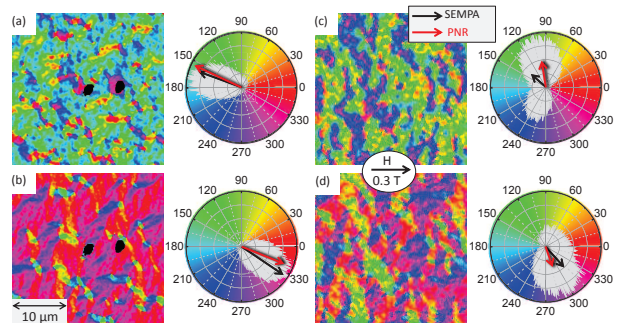


FIG. 4: (color online) SEMPA images of the magnetization in the top (a,c) and bottom (b,d) layers before (a,b) and after (c,d) an applied field of 0.3 T. Polar histograms to the right of each figure show the distribution (in grey) of magnetization angles in the image. The average magnetization from the image (black arrow) and the magnetization measured using PNR (red arrow) are also shown.

A 0.3 T field was then applied along the sample edge (at  $0^\circ$  in Fig. 4), and the PNR and SEMPA remanent state measurements were repeated (Figs. 3b, 4c and 4d). The specular reflectivity shows a pronounced increase in the SF scattering relative to the as-grown state (Fig. 3a) indicating that the projections of the layer magnetizations perpendicular to the field have increased, and

the  $R^{++}$  and  $R^{--}$  NSF cross sections are now essentially equal. The red arrows in Fig. 4c) and d), obtained from the PNR fits, show that the net magnetization of each layer has rotated in opposite directions away from the applied field, consistent with a spin flop transition. The PNR analysis also indicates that the magnitudes of the Co net layer magnetizations are reduced from their as-grown values, indicative of a decrease in average domain size. These measurements complement the SEMPA measurements performed on another  $1\text{ mm}^2$  area of the sample. The SEMPA images in Figs. 4c) and 4d) show that the field induces a more complicated remanent magnetic structure, with a bimodal domain distribution within each layer that is tilted away from the applied field. These SEMPA data are consistent with a relaxed scissor state induced by a spin-flop transition. A comparison between top and bottom Co layers in both the SEMPA and PNR results shows that they are still antiferromagnetically coupled. (The PNR data show no direct evidence of the bimodal distribution because the reflectivity the Co-bilayer spin configuration shown in Figs. 4c and 4d is nearly identical to that for the configuration that is mirror symmetric about the field. The actual spin state is clearly a linear combination of these two.) Also, SEMPA and PNR measurements on similar samples containing F' layers of Ni or PdNi confirm that the remanent magnetizations of those layers point in the direction of  $H_{app}$  after application of 0.3 T.

The PNR and SEMPA measurements reveal that the evolution of the magnetic structures within the SAF is complex, but is consistent with a spin-flop transition. While this transition explains the field-induced spin-triplet supercurrent enhancement, it is notable that the state has multiple in-plane domains and the Co layer magnetizations are tilted slightly from the direction perpendicular to the applied field.

In conclusion, we have observed a large enhancement of the spin-triplet supercurrent in S/F'/SAF/F'/S Josephson junctions when the F' layers are magnetized by an applied field and the SAF undergoes a spin-flop transition. This result confirms the theoretical prediction that the spin-triplet supercurrent is maximum when the magnetizations of the adjacent ferromagnetic layers inside the junctions are aligned perpendicular to each other. This result also underscores the need for characterization and control of the magnetic structure to optimize the performance of spin-triplet S/F/S devices. This could be done in the future by a number of methods, e.g. by exploiting shape anisotropy or by using magnetic materials with perpendicular-to-plane anisotropy.

**Acknowledgments:** We acknowledge helpful conversations with Mark Stiles and Bob McMichael. We also thank R. Loloee and B. Bi for technical assistance, and use of the W.M. Keck Microfabrication Facility. This work was supported by the U.S. Department of Energy under grant DE-FG02-06ER46341.

---

\* Electronic address: birge@pa.msu.edu

† Present address: Physics Department, Juniata College, Huntingdon, PA 16652, USA.

- [1] A.I. Buzdin, *Rev. Mod. Phys.* **77** 935 (2005).
- [2] E.A. Demler, G.B. Arnold, and M.R. Beasley, *Phys. Rev. B* **55**, 15174 (1997).
- [3] F.S. Bergeret, A.F. Volkov, and K.B. Efetov, *Phys. Rev. B* **64**, 134506 (2001).
- [4] A.P. Mackenzie, and Y. Maeno, *Rev. Mod. Phys.* **75**, 657 (2003).
- [5] S.S. Saxena et al. *Nature* **406**, 587 (2000).
- [6] F.S. Bergeret, A.F. Volkov, and K.B. Efetov, *Phys. Rev. Lett.* **86**, 4096 (2001).
- [7] A. Kadigrobov, R.I. Shekhter, and M. Jonson, *Europhys. Lett.* **54**(3), 394 (2001).
- [8] M. Eschrig, J. Kopu, J.C. Cuevas, and Gerd Schön, *Phys. Rev. Lett.* **90**, 137003 (2003).
- [9] R.S. Keizer, S.T.B. Goennenwein, T.M. Klapwijk, G. Miao, G. Xiao, and A. Gupta, *Nature (London)* **439**, 825 (2006).
- [10] I. Sosnin, H. Cho, V.T. Petrashov, and A.F. Volkov, *Phys. Rev. Lett.* **96**, 157002 (2006).
- [11] T.S. Khaire, M.A. Khasawneh, W.P. Pratt Jr. and N.O. Birge, *Phys. Rev. Lett.* **104**, 137002 (2010).
- [12] J.W.A. Robinson, J.D.S. Witt and M.G. Blamire, *Science* **329**, 59 (2010).
- [13] D. Sprungmann, K. Westerholt, H. Zabel, M. Weides and H. Kohlstedt, *Phys. Rev. B* **82**, 060505 (2010).
- [14] M. S. Anwar, F. Czeschka, M. Hesselberth, M. Porcu, and J. Aarts, *Phys. Rev. B* **82**, 100501 (2010).
- [15] M. Houzet and A.I. Buzdin, *Phys. Rev. B* **76**, 060504(R) (2007).
- [16] J.-G. Zhu and Y. Zheng, *IEEE Trans. Mag.* **34**, 1063 (1998).
- [17] H.C. Tong, C. Qian, L. Miloslavsky, S. Funada, X. Shi, F. Liu, and S. Dey, *J. Appl. Phys.* **87**, 5055 (2000).
- [18] M.A. Khasawneh, T.S. Khaire, C. Klose, W.P. Pratt Jr. and N.O. Birge, *Supercond. Sci. Technol.* **24**, 024005 (2011).
- [19] M.A. Khasawneh, W.P. Pratt Jr. and N.O. Birge, *Phys. Rev. B* **80**, 020506(R) (2009).
- [20] O. Bourgeois, P. Gandit, J. Lesueur, A. Sulpice, X. Grison, and J. Chaussy, *Eur. Phys. J. B* **21**, 75 (2001).
- [21] T.S. Khaire, W.P. Pratt, Jr., and N.O. Birge, *Phys. Rev. B* **79**, 094523 (2009).
- [22] The shift of the Fraunhofer pattern after magnetizing an S/F/S Josephson junction was first reported by V.V. Ryazanov, *Physics-Uspekhi* **42**, 825 (1999). The calculation of the field shift is given in [21].
- [23] A.F. Volkov and K.B. Efetov, *Phys. Rev. B* **81** 144522 (2010).
- [24] L. Trifunovic and Z. Radovic, *Phys. Rev. B* **82** 020505(R)(2010).
- [25] J. A. Borchers, J. A. Dura, J. Unguris, D. Tulchinsky, M. H. Kelley, C. F. Majkrzak, S. Y. Hsu, R. Loloee, W. P. Pratt, and J. Bass, *Phys. Rev. Lett.* **82**, 2796 (1999).
- [26] P.A. Kienzle, K.V. O'Donovan, J.F. Ankner, N.F. Berk, C.F. Majkrzak, <http://www.ncnr.nist.gov/reflpak> (2000-2006).